

# Microstructure evolution and magnetoresistance of the A-site ordered Ba-doped manganites

© S.V. Trukhanov<sup>†</sup>, L.S. Lobanovski, M.V. Bushinsky, V.A. Khomchenko,  
V.V. Fedotova, I.O. Troyanchuk, H. Szymczak\*

Joint Institute of Solids and Semiconductor Physics, National Academy of Sciences of Belarus,  
220072 Minsk, Belarus

\* Institute of Physics, Polish Academy of Sciences,  
02-668 Warsaw, Poland

(Получена 12 сентября 2006 г. Принята к печати 3 октября 2006 г.)

The microstructure, crystal structure and magnetotransport properties of the micro-sized and nano-sized Ba-doped manganites have been investigated. „Two-step“ reduction-reoxidation procedure has been used to obtain nano-sized ceramic manganite  $\text{Nd}_{0.70}\text{Ba}_{0.30}\text{MnO}_3$  (II). The parent micro-sized manganite  $\text{Nd}_{0.70}\text{Ba}_{0.30}\text{MnO}_3$  (I) have been prepared by usual ceramic technology in air. Then the sample has been annealed in vacuum. The grain size of the reduced sample, determined by scanning electron microscopy, decreased from  $\sim 5 \mu\text{m}$  down to  $\sim 100 \text{nm}$ . To obtain the oxygen stoichiometry nano-sized sample, the  $\text{Nd}_{0.70}\text{Ba}_{0.30}\text{MnO}_{2.60}$  has been again annealed in air. It is established that the (I) sample is a pseudocubic perovskite whereas (II) — a tetrahedral as consequence of  $\text{Nd}^{3+}$  and  $\text{Ba}^{2+}$  ions as well as oxygen vacancies ordering. The (I) sample is ferromagnet with  $T_C \approx 140 \text{K}$ . It has metal–insulator transition at  $T_{MI} \approx 135 \text{K}$  and peak of magnetoresistance  $\sim 50\%$  in field of 9 kOe. For the (II) sample the critical points of phase transitions move to higher temperatures,  $T_C \approx 320 \text{K}$  and  $T_{MI} \approx 310 \text{K}$ . The magnetoresistance of the (II) sample at the room temperature ( $T \approx 293 \text{K}$ ) is about 7% in field of 9 kOe. The magnetotransport properties are interpreted in frame of nano-sized effect.

PACS: 75.30.Et, 75.30.Vn, 75.50.Lk

## 1. Introduction

The layered  $\text{L}\text{BaMn}_2\text{O}_{6-\gamma}$  ( $\text{L} = \text{La}, \text{Pr}, \text{Nd}$  et al.) manganites have been found to possess unique physical properties, which is related to the ordering of cations in A-sublattice of the perovskite structure [1–16]. The main structural feature of these A-site ordered compounds consists in the alternation of  $\text{MnO}_2$  plane with two other planes  $\text{LO}$  and  $\text{BaO}$ , each containing cations of one type which results in a periodic distortion of  $\text{MnO}_6$  octahedra. This crystal structure is similar to that of  $\text{YBaCuFeO}_5$  [17]. The physical properties of such A-site ordered  $\text{L}\text{BaMn}_2\text{O}_6$  manganites cannot be explained taking into account the tolerance factor alone, as in the case of a statistical distribution of substituent cations in manganites of the  $\text{L}_{0.50}\text{Ba}_{0.50}\text{MnO}_3$  type. This type of cation ordering increases the temperature of the phase transition from a metallic ferromagnetic state to an insulator paramagnetic state. In the case of  $\text{L}^{3+} = \text{Pr}^{3+}$  the Curie temperature increases from  $\sim 140$  to  $\sim 320 \text{K}$  [18]. In both the disordered and ordered cases, the MR effect is observed at temperatures slightly below  $T_C$ .

Recently, the manganites with  $\text{L}^{3+}/\text{Ba}^{2+} \neq 1/1$  cation ratio have been investigated [8]. The ferromagnetic properties in ground state have been observed for the A-site ordered  $\text{La}_{1-x}\text{Ba}_x\text{MnO}_3$  samples with  $x = 0.44, 0.48$ . The ferromagnetic and antiferromagnetic properties have been observed for the sample with  $x = 0.52$ . For the  $x = 0.50$  sample, neutron powder diffraction data provide evidence for a structural phase separation below  $\sim 180 \text{K}$  and a stable and complex antiferromagnetic charge ordered phase

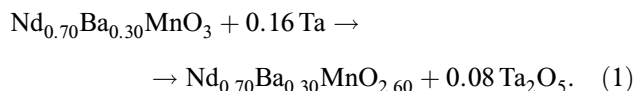
at temperatures below  $\sim 120 \text{K}$ . For the  $x = 0.52$  sample, a similar charge ordered state has been observed within a narrow temperature range at  $\sim 180 \text{K}$  before it disappeared in favor of a more stable antiferromagnetic A-type orbital ordered phase [19]. So it is very interesting to study the mechanism of the A-site ordering and magnetic properties of the manganites with  $\text{L}^{3+}/\text{Ba}^{2+} \gg 1$  cation ratio. In present paper we have selected the  $\text{Nd}_{0.70}\text{Ba}_{0.30}\text{MnO}_3$  solid solution. The granular size effect on the magnetotransport properties of the A-site ordered manganites is also curious. It is observed [20] by the Rietveld analysis of the powder X-ray diffraction data of the phase-pure nanopowders  $\text{La}_{0.67}\text{Ca}_{0.33}\text{MnO}_3$  that the particle size reduction leads to a significant contraction of the unit cell volume and a resuction of the unit cell anisotropy. We propose that these two effects A-site ordering and formation of nano-sized granules are responsible for the observed enhancement in  $T_C$ .

## 2. Experimental section

The starting A-site disordered  $\text{Nd}_{0.70}\text{Ba}_{0.30}\text{MnO}_3$  (I) manganite has been obtained from high purity oxides and carbonate:  $\text{Nd}_2\text{O}_3$ ,  $\text{Mn}_2\text{O}_3$  and  $\text{BaCO}_3$ . At first the oxides and carbonate have been mixed with design ( $\text{Nd}^{3+} : \text{Ba}^{2+} : \text{Mn}^{3+} = 7 : 3 : 10$ ) cation ratio and ground thoroughly in an agate mortar by adding some quantity of ethyl alcohol. Then the preforming has been performed at  $1000^\circ\text{C}$  in air during 2 h to remove a moisture and carbonic acid. Final synthesis has been carried out at  $1550^\circ\text{C}$  in air during 2 h. After synthesis the samples have been slowly cooled  $100^\circ\text{C} \cdot \text{h}^{-1}$  in order to receive the stoichiometric

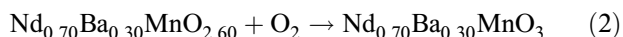
<sup>†</sup> E-mail: trukhanov@ifftp.bas-net.by

oxygen content. The air-prepared  $\text{Nd}_{0.70}\text{Ba}_{0.30}\text{MnO}_3$  sample has been treated in an evacuated soldered silica tube at  $800^\circ\text{C}$  during 24 h using Ta as oxygen getter down to „ $\text{O}_{2.60}$ “ state:



The anion-deficient  $\text{Nd}_{0.70}^{3+}\text{Ba}_{0.30}^{2+}\text{Mn}_{0.50}^{3+}\text{O}_{2.60}^{2-}$  sample is characterized by the partly ordered  $\text{Nd}^{3+}$  and  $\text{Ba}^{2+}$  cation location and the pyramidal  $\text{Mn}^{2+}/\text{Mn}^{3+}$  layers, sandwiched between alternating  $\text{Nd}^{3+}$  oxygen-free and  $\text{Ba}^{2+}$  oxygen-filled layers along the [001] axis. To lower a relative error of oxygen content measurements the weight of the sample placed in silica tube has been  $\sim 3$  g.

The anion-deficient A-site ordered  $\text{Nd}_{0.70}\text{Ba}_{0.30}\text{MnO}_{2.60}$  sample has been oxidized in air at  $800^\circ\text{C}$  during 8 h up to the oxygen-stoichiometric „ $\text{O}_3$ “ state, where the A-site ordering remains:



So two step reduction-reoxidation procedure has been used to obtain nanosized ceramic manganite  $\text{Nd}_{0.70}\text{Ba}_{0.30}\text{MnO}_3$  (II). The microstructure of all the obtained samples has been studied by NANOLAB-7 scanning electron microscope. The quantitative chemical content and its spatial distribution have been examined by the MS-46 and SYSTEM-860-500 microprobes. These investigations have shown that all the obtained samples are well crystallized with homogeneous chemical content. The oxygen content of all the products has been determined by thermogravimetric analysis. So the chemical formula for all the examined samples may be written as  $\text{Nd}_{0.70}\text{Ba}_{0.30}\text{MnO}_{3-\delta \pm 0.01}$ . X-ray powder diffraction data have been recorded at room temperature with a DRON-3M diffractometer in  $\text{Cu-K}\alpha$  radiation in angle range  $20^\circ \leq 2\theta \leq 80^\circ$ . The magnetization measurements have been made using an OI-3001 commercial vibrating sample magnetometer in the temperature range 4.2–350 K. The temperature dependences of the specific magnetization have been measured in weak field during heating after field cooling (FC) mode. The Curie temperature ( $T_C$ ) has been defined as an inflection point of the FC magnetization. The resistivity was studied in a temperature interval from 77 to 350 K using the standard four-point-probe technique and the samples with ultrasonically applied indium eutectic contacts. The negative isotropic MR has determined as:

$$\text{MR} = \{[\rho(H) - \rho(0)]/\rho(0)\} \cdot 100\% \quad (3)$$

where  $\rho(H)$  and  $\rho(0)$  are the resistivities measured in a magnetic field of  $H = 9$  kOe and in the absence of an applied magnetic field.

### 3. Experimental results and discussion

The microstructure investigations have shown that the as-prepared  $\text{Nd}_{0.70}\text{Ba}_{0.30}\text{MnO}_3$  (I) sample has well crystallized grains with average diameter  $\langle D \rangle \approx 5 \mu\text{m}$  (Fig. 1, a). The

grains exhibit a certain size distribution. It is established that the annealing of the as-prepared sample in the reductive  $P[\text{O}_2] \approx 10^{-4}$  Pa atmosphere at the moderate  $T = 800$  K temperature up to nominal composition  $\text{Nd}_{0.70}\text{Ba}_{0.30}\text{MnO}_{2.60}$  leads to the degradation of the ceramic and the formation of nanometric  $\langle D \rangle \approx 100$  nm grains (Fig. 1, b). It is probably the appearance of the oxygen vacancies and intensive cation exchange destroy the initial grains. The nanograins combine to form a certain mosaic structure, which is common for the entire polycrystalline sample. The grain size determines, to a certain extent, the properties of the crystal structure. A decrease in the grain size to the nanodimensional level is accompanied by a certain decrease in the unit cell volume, which is explained by an increase in the forces of surface tension relative to the bulk elastic forces [21].

The oxidation of the anion-deficient A-site ordered  $\text{Nd}_{0.70}\text{Ba}_{0.30}\text{MnO}_3$  sample in the air at the moderate  $T = 800$  K temperature leads to the formation of the oxygen-stoichiometric A-site ordered  $\text{Nd}_{0.70}\text{Ba}_{0.30}\text{MnO}_3$  (II) one and does not change of the nanometric dimension of

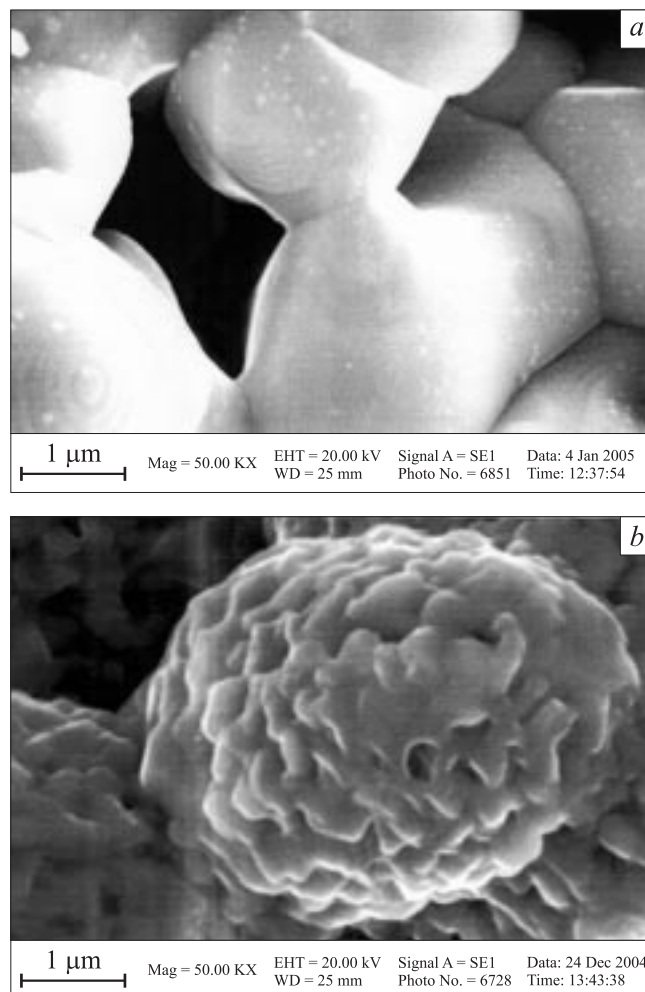


**Figure 1.** The scanning electron micrographs: *a* — for the micro-sized  $\text{Nd}_{0.70}\text{Ba}_{0.30}\text{MnO}_3$  and *b* — for nanosized  $\text{Nd}_{0.70}\text{Ba}_{0.30}\text{MnO}_3$  samples.

the grains. It should be noted the diminution of the grain average diameter leads to two competitive processes: 1) the weakening of the ferromagnetic properties owing to distortion of the exchange interactions on the grain surface [22,23] and 2) the strengthening of the ferromagnetic properties owing to compression of the unit cell under the influence of the surface forces [24,25]. In extreme case the former leads to the formation of the spin glass state, while the latter leads to the increase of  $T_C$ .

The powder X-ray diffraction results have demonstrated that the as-prepared  $\text{Nd}_{0.70}\text{Ba}_{0.30}\text{MnO}_3$  (I) sample has an pseudocubic unit cell. No additional reflections indicating a presence of impurity structural phases have been detected. The parameter of the unit cell for (I) sample is  $a = 3.884 \text{ \AA}$ . The crystal structure of the oxygen-stoichiometric  $A$ -site ordered  $\text{Nd}_{0.70}\text{Ba}_{0.30}\text{MnO}_3$  (II) sample can be described by a tetragonal perovskite phase with parameters  $a = 3.889 \text{ \AA}$  and  $c = 7.731 \text{ \AA}$ . The tetragonal symmetry is in agreement with the  $\text{Nd}^{3+}$  and  $\text{Ba}^{2+}$  cation ordering on the  $A$ -site of the perovskite cell.

It should be noted that the unit cell volume of the anion-deficient  $A$ -site ordered phase much larger one than for the as-prepared phase. This is caused by increasing manganese ion size as result of its oxidative state decrease  $\text{Mn}^{3+} \rightarrow \text{Mn}^{2+}$ , although an appearance of oxygen vacan-

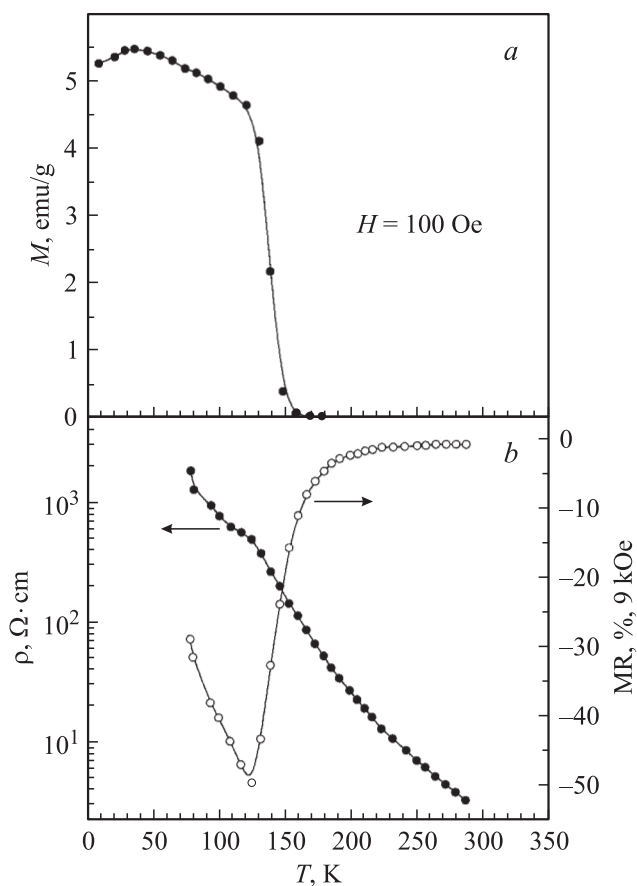


**Figure 2.** *a* — FC magnetization and *b* — resistivity with magnetoresistance vs. temperature for the micro-sized  $\text{Nd}_{0.70}\text{Ba}_{0.30}\text{MnO}_3$  sample.

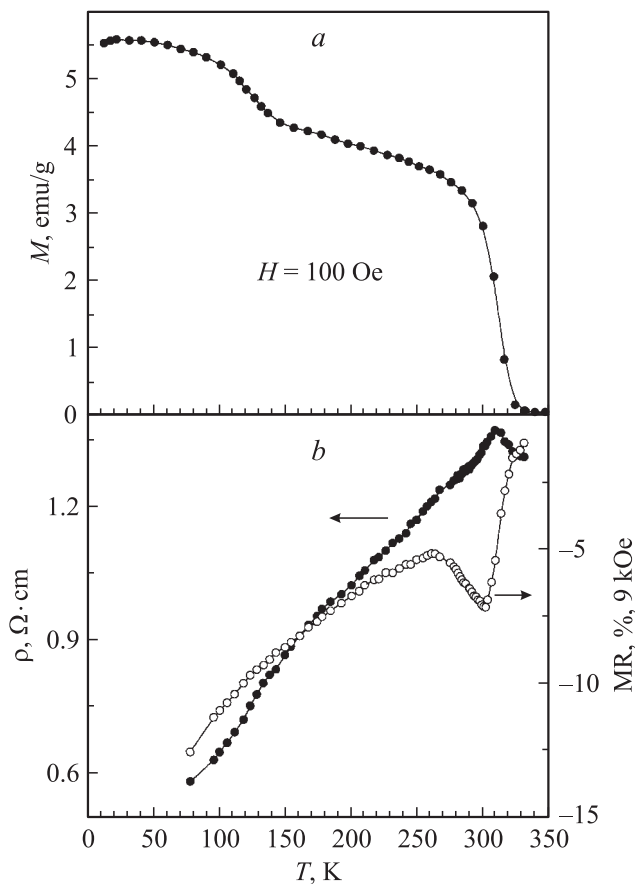


**Figure 3.** *a* — FC magnetization and *b* — resistivity with magnetoresistance vs. temperature for the nano-sized  $\text{Nd}_{0.70}\text{Ba}_{0.30}\text{MnO}_3$  sample.

cies and decreasing coordination number of manganese ions have to decrease of the unit cell volume. It is well known that  $\text{Mn}^{3+}$  (HS) effective ionic radius in octahedral oxygen coordination is  $0.645 \text{ \AA}$ , while it in pentahedral one —  $0.580 \text{ \AA}$  [26]. For the  $\text{Mn}^{2+}$  (HS) ions the effective ionic radii are following  $0.830$  and  $0.750 \text{ \AA}$  for the octahedral and pentahedral coordination, respectively. The oxygen-stoichiometric  $A$ -site ordered phase has the unit cell volume smaller than one for the as-prepared phase. This compression of the unit cell may be explained by the ordering of the  $A$  cations and the formation of the nanograins. The compression of the unit cell produces the enhancement of the exchange interactions as a result of lessening of average  $\langle \text{Mn-O} \rangle$  bond length and increasing of average  $\langle \text{Mn-O-Mn} \rangle$  bond angle.

The results of the FC magnetization as well as magnetotransport measurements vs. temperature for the (I) and (II) samples are presented in Fig. 2 and 3. The as-prepared  $\text{Nd}_{0.70}\text{Ba}_{0.30}\text{MnO}_3$  (I) sample is characterized by the Curie temperature  $\sim 140 \text{ K}$  (Fig. 2, *a*). The transition to a paramagnetic state is well defined, which is characteristic of homogeneous magnetic materials. The (I) sample have an insulator type of the electrical resistivity and insulator–metal transition at  $135 \text{ K}$  (Fig. 2, *b*). At this

temperature in field of 9 kOe the peak of magnetoresistance of  $\sim 50\%$  is observed.

The oxygen-stoichiometric A-site ordered  $\text{Nd}_{0.70}\text{Ba}_{0.30}\text{MnO}_3$  (II) sample has Curie temperature  $\sim 310$  K, which is more than two times as large as for the as-prepared sample (Fig. 3, a). It is well shown that the (II) sample has one more magnetic transitions at low temperature  $\sim 120$  K. For the (II) sample the peak of magnetoresistance of  $\sim 7\%$  in field of 9 kOe is observed around 310 K (Fig. 3, b).

For the (II) sample the spontaneous magnetic moment is  $\sim 3.0 \mu_B/\text{f.u.}$  that is some below than one for the as-prepared (I) sample. This fact is explained by the formation of nanograins. On the surface of grain the exchange interactions are distorted and total magnetic moment decreases. In the case of nanograins this is especially visible.

Nanosized effect produces the reduction of the unit cell and as consequence the increase of intensity of exchange interactions between  $\text{Mn}^{3+}$  and  $\text{Mn}^{4+}$  ions [27]. We have to underline that nanosized effect on magnetotransport properties of manganites is similar to external hydrostatic pressure one. This is remarkable result since this materials is potential candidate for the use as information storage device operating at the room temperature.

#### 4. Conclusion

The high-quality ceramic  $\text{Nd}_{0.70}\text{Ba}_{0.30}\text{MnO}_3$  with the controlled chemical phase content and microstructure has been obtained. It is established that the annealing in the reduction  $P[\text{O}_2] \approx 10^{-4}$  Pa atmosphere at the moderate  $T = 800$  K temperature leads to the degradation of this ceramic and the formation of nanometric  $\langle D \rangle \approx 100$  nm grains. The A-site ordered manganites with  $\text{Nd}^{3+}/\text{Ba}^{2+} \gg 1$  cation ratio may be obtained using „two-step“ reduction-reoxidation method at the moderate  $T = 800$  K temperature. The A-site ordering and the formation of nanometric grains leads to considerable changes of the crystal structure and the increase of the Curie temperature. It is established that the  $\text{Nd}_{0.70}\text{Ba}_{0.30}\text{MnO}_3$  (I) sample is a pseudocubic perovskite whereas  $\text{Nd}_{0.70}\text{Ba}_{0.30}\text{MnO}_3$  (II) — a tetrahedral as consequence of  $\text{Nd}^{3+}$  and  $\text{Ba}^{2+}$  ions as well as oxygen vacancies ordering. The (I) sample is ferromagnet with  $T_C \approx 140$  K. It has metal–insulator transition at  $T_{\text{MI}} \approx 135$  K and peak magnetoresistance  $\sim 50\%$  in field of 9 kOe. For the (II) sample the critical points of phase transitions move to higher temperatures,  $T_C \approx 320$  K and  $T_{\text{MI}} \approx 310$  K. The magnetoresistance of the (II) sample at the room temperature ( $T \approx 293$  K) is about 7% in field of 9 kOe. Such considerable changes of the crystal structure and magnetic properties are interpreted in frame of the A-site ordering and the formation of nanometric grains.

The work was partly supported by the Belarus Fund for Basic Research (F06R-078) and the State Committee for Scientific Research (Poland) (Grant no. KBN 1 P03B 038 27).

#### References

- [1] A.A. Taskin, A.N. Lavrov, Y. Ando. Appl. Phys. Lett., **86**, 091 910 (2005).
- [2] J. Spooen, R.I. Walton, F. Millange. J. Mater. Chem., **15**, 1542 (2005).
- [3] C. Perca, L. Pinsard-Gaudart, A. Daoud-Aladine. Chem. Mater., **17**, 1835 (2005).
- [4] N. Furukawa, Y. Motome. J. Phys. Soc. Jap., **74**, S203 (2005).
- [5] T. Nakajima, Y. Ueda. J. Appl. Phys., **98**, 046 108 (2005).
- [6] Q. Zhang, W. Zhang, Z. Jiang. Phys. Rev. B, **72**, 144 415 (2005).
- [7] A.J. Williams, J.P. Attfield. Phys. Rev. B, **72**, 024 436 (2005).
- [8] O. Chmaissem, B. Dabrowski, S. Kolesnik, J. Mais, J.D. Jorgensen, S. Short, C.E. Botez, P.W. Stephens. Phys. Rev. B, **72**, 104 426 (2005).
- [9] S.V. Trukhanov. JETP, **101**, 513 (2005).
- [10] A.J. Williams, J.P. Attfield, S.A.T. Redfern. Phys. Rev. B, **72**, 184 426 (2005).
- [11] Y. Ueda, T. Nakajima. Progr. Theor. Phys., **159**, 365 (2005).
- [12] T. Ohno, H. Kubo, Y. Kawasaki, Y. Kishimoto, T. Nakajima, Y. Ueda. Physica B, **359-361**, 1291 (2005).
- [13] S.V. Trukhanov, L.S. Lobanovski, M.V. Bushinsky, V.V. Fedotova, I.O. Troyanchuk, A.V. Trukhanov, V.A. Ryzhov, H. Szymczak, R. Szymczak, M. Baran. J. Phys.: Condens. Matter., **17**, 6495 (2005).
- [14] Y. Kawasaki, T. Minami, Y. Kishimoto, Y. Kishimoto, T. Nakajima, Y. Ueda. Phys. Rev. Lett., **96**, 037 202 (2006).
- [15] S.V. Trukhanov, A.V. Trukhanov, H. Szymczak, R. Szymczak, M. Baran. J. Phys. Chem. Sol., **67**, 675 (2006).
- [16] T. Nakajima, T. Yamauchi, J. Yamaura, Y. Ueda. J. Phys. Chem. Sol., **67**, 620 (2006).
- [17] L. Er-Rakho, C. Michel, Ph. Lacorre, B. Raveau. J. Sol. St. Chem., **73**, 531 (1988).
- [18] S.V. Trukhanov, I.O. Troyanchuk, M. Hervieu, H. Szymczak, K. Bärner. Phys. Rev. B, **66**, 184 424 (2002).
- [19] T. Nakajima, H. Yoshizawa, Y. Ueda. J. Phys. Soc. Jap., **73**, 2283 (2004).
- [20] K.S. Shankar, S. Kar, G.N. Subbanna, A.K. Raychaudhuri. Sol. St. Commun., **129**, 479 (2004).
- [21] S.V. Trukhanov, L.S. Lobanovski, M.V. Bushinsky, V.A. Khomchenko, N.V. Pushkarev, I.O. Troyanchuk, A. Maignan, D. Flahaut, H. Szymczak, R. Szymczak. Eur. Phys. J. B, **42**, 51 (2004).
- [22] N. Zhang, W. Yang, W. Ding, D. Xing, Y. Du. Sol. St. Commun., **109**, 537 (1999).
- [23] G. Pang, X. Xu, V. Markovich, S. Avivi, O. Palchik, Y. Koltypin, G. Gorodetsky, Y. Yeshurun, H.P. Buchkremer, A. Geranken. Mater. Res. Bulletin, **38**, 11 (1999).
- [24] K. Uchino, E. Sadanaga, T. Hirose. J. Am. Ceram. Soc., **72**, 1555 (1989).
- [25] S. Chattopadhyay, P. Ayyub, V.R. Palkar, A.V. Gurjar, R. Wankar, M. Multani. J. Phys.: Condens. Matter., **9**, 8135 (1997).
- [26] R.D. Shannon. Acta Crystallog. A, **32**, 751 (1976).
- [27] S.V. Trukhanov, L.S. Lobanovski, M.V. Bushinsky, I.O. Troyanchuk, H. Szymczak. J. Phys.: Condens. Matter., **15**, 1783 (2003).

Редактор Л.В. Беляков